


Hyperpolarized ^{13}C MR Spectroscopy Depicts in Vivo Effect of Exercise on Pyruvate Metabolism in Human Skeletal Muscle

Jae Mo Park, PhD • Crystal E. Harrison, PhD • Junjie Ma, BS • Jun Chen, PhD • James Ratnakar, PhD • Zunguo Zun, PhD • Jeff Liticker, PharmD • Galen D. Reed, PhD • Avneesh Chhabra, MD • Ronald G. Haller, MD • Thomas Jue, PhD • Craig R. Malloy, MD

From the Advanced Imaging Research Center (J.M.P., C.E.H., J.M., J.C., J.R., J.L., G.D.R., A.C., C.R.M.), Department of Radiology (J.M.P., A.C., C.R.M.), Department of Neurology and Neurotherapeutics (R.G.H.), and Department of Internal Medicine (C.R.M.), University of Texas Southwestern Medical Center, 5323 Harry Hines Blvd, Dallas, TX 75390-8568; Department of Electrical and Computer Engineering, University of Texas at Dallas, Dallas, Tex (J.M.P.); Department of Diagnostic Imaging and Radiology, Developing Brain Institute, Children's National Hospital, Washington, DC (Z.Z.); Department of Pediatrics and Radiology, George Washington University, Washington, DC (Z.Z.); GE Healthcare, Dallas, Tex (G.D.R.); Department of Biochemistry and Molecular Medicine, University of California, Davis, Calif (T.J.); and Veterans Affairs North Texas Healthcare System, Dallas, Tex (C.R.M.). Received December 7, 2020; revision requested February 1, 2021; revision received April 1; accepted April 22. **Address correspondence to** J.M.P. (e-mail: Jaemo.Park@utsouthwestern.edu).

This study was funded by the National Institutes of Health (R01 NS107409, P41 EB015908, S10 RR029119, S10 OD018468, and R01 HD100012), the Welch Foundation (I-2009-20190330), the Texas Institute for Brain Injury and Repair, and the University of Texas at Dallas Collaborative Biomedical Research Award (UTD 1907789).

Conflicts of interest are listed at the end of this article.

Radiology 2021; 300:626–632 • <https://doi.org/10.1148/radiol.2021204500> • Content codes: 

Background: Pyruvate dehydrogenase (PDH) and lactate dehydrogenase are essential for adenosine triphosphate production in skeletal muscle. At the onset of exercise, oxidation of glucose and glycogen is quickly enabled by dephosphorylation of PDH. However, direct measurement of PDH flux in exercising human muscle is daunting, and the net effect of covalent modification and other control mechanisms on PDH flux has not been assessed.

Purpose: To demonstrate the feasibility of assessing PDH activation and changes in pyruvate metabolism in human skeletal muscle after the onset of exercise using carbon 13 (^{13}C) MRI with hyperpolarized (HP) [$1\text{-}^{13}\text{C}$]-pyruvate.

Materials and Methods: For this prospective study, sedentary adults in good general health (mean age, 42 years \pm 18 [standard deviation]; six men) were recruited from August 2019 to September 2020. Subgroups of the participants were injected with HP [$1\text{-}^{13}\text{C}$]-pyruvate at resting, during plantar flexion exercise, or 5 minutes after exercise during recovery. In parallel, hydrogen 1 arterial spin labeling MRI was performed to estimate muscle tissue perfusion. An unpaired *t* test was used for comparing ^{13}C data among the states.

Results: At rest, HP [$1\text{-}^{13}\text{C}$]-lactate and [$1\text{-}^{13}\text{C}$]-alanine were detected in calf muscle, but [^{13}C]-bicarbonate was negligible. During moderate flexion-extension exercise, total HP ^{13}C signals (tC) increased 2.8-fold because of increased muscle perfusion ($P = .005$), and HP [$1\text{-}^{13}\text{C}$]-lactate-to-tC ratio increased 1.7-fold ($P = .04$). HP [^{13}C]-bicarbonate-to-tC ratio increased 8.4-fold ($P = .002$) and returned to the resting level 5 minutes after exercise, whereas the lactate-to-tC ratio continued to increase to 2.3-fold as compared with resting ($P = .008$).

Conclusion: Lactate and bicarbonate production from hyperpolarized (HP) [$1\text{-}^{13}\text{C}$]-pyruvate in skeletal muscle rapidly reflected the onset and the termination of exercise. These results demonstrate the feasibility of imaging skeletal muscle metabolism using HP [$1\text{-}^{13}\text{C}$]-pyruvate MRI and the sensitivity of in vivo pyruvate metabolism to exercise states.

©RSNA, 2021

Online supplemental material is available for this article.

A continuous supply of adenosine triphosphate is required for contracting skeletal muscle. Aside from transient buffering by the phosphocreatine pool, adenosine triphosphate must be generated either with substrate-level phosphorylation during metabolism of glucose to lactate or with oxidative phosphorylation, which depends on the metabolism of acetyl coenzyme A in the tricarboxylic acid cycle. Pyruvate dehydrogenase (PDH) regulates carbohydrates, as opposed to fatty acids, as the source of acetyl coenzyme A during exercise (1), and it determines the fraction of energy derived from glycogen and/or glucose and fatty acids. Dephosphorylation of PDH generates the active form after the onset of exercise (2,3), but the PDH activation rate in vivo remains

poorly determined. Consequently, the early effect of exercise on PDH flux in human muscle is unknown and presumably depends on allosteric modulators. PDH plays a central role in normal physiologic findings and displays altered activity as the physiologic characteristics change. For example, PDH flux capacity diminishes with age (4). PDH decreases in type 2 diabetes skeletal muscle (5). PDH activity in skeletal muscle is disrupted in congenital defects of the PDH complex (6–8) and in mitochondrial myopathies.

Intermediary metabolism in skeletal muscle has been investigated in isolated preparations or tissue biopsies (3,9). In vivo studies of fuel utilization are feasible but require invasive arterial and venous blood samplings. The hyperpolarized

Abbreviations

HP = hyperpolarized, PDH = pyruvate dehydrogenase, tC = total HP carbon 13 signals

Summary

This study demonstrates the feasibility of imaging skeletal muscle metabolism using hyperpolarized carbon 13 pyruvate MRI and the sensitivity of in vivo pyruvate metabolism to exercise states.

Key Results

- In a prospective study of nine healthy adults undergoing MRI, total hyperpolarized carbon 13 (^{13}C) signals (tC) in calf muscle increased 2.8-fold during plantar flexion exercise due to increased perfusion ($P = .005$) compared with resting.
- $[1-^{13}\text{C}]$ -Lactate-to-tC ratio increased 1.7-fold during exercise ($P = .04$) and 2.3-fold during recovery (5 minutes after exercise, $P = .008$) compared with resting.
- $[^{13}\text{C}]$ -Bicarbonate-to-tC ratio increased 8.4-fold during exercise ($P = .002$), returning to resting level ($P = .21$) during recovery.

(HP) carbon 13 (^{13}C) technique has been introduced to detect enzyme-catalyzed reactions, such as PDH and lactate dehydrogenase in human prostate cancer and the heart, using $[1-^{13}\text{C}]$ -pyruvate (10,11). Unlike the highly oxidative tissues of the heart and brain, adenosine triphosphate demand and flux through energy-generating pathways is very low in skeletal muscle at rest (1). During modest exercise, glycogen oxidation and PDH flux increase dramatically. PDH is a key contributing enzyme to energy production. The contribution of blood-borne substrates is highly variable and depends on nutritional state, duration and intensity of exercise, and other factors (12,13). HP studies have followed the rapid activation of PDH in rodent muscle using a pyruvate dehydrogenase kinase inhibitor or electrical stimulations (14,15), but applications in human skeletal muscle have not been explored. This study demonstrates that production of $[^{13}\text{C}]$ -bicarbonate and $[1-^{13}\text{C}]$ -lactate from HP $[1-^{13}\text{C}]$ -pyruvate in human skeletal muscle is sensitive to brief exercise using validated protocols for MRI studies of human muscle energetics (16–19).

Materials and Methods

Study Protocol

The protocol of this prospective study was approved by the local institutional review board (institutional review board no. STU-2018–0227) and was performed from August 2019 to September 2020. Nine volunteers (mean age, 42 years \pm 18 [standard deviation]; six men, three women) (Table 1) were recruited by word of mouth. Informed written consent was obtained from all participants. The study participants were sedentary adults in good general health with no history of peripheral vascular, systemic, cardiac, or musculoskeletal disease. The study was compliant with the Health Insurance Portability and Accountability Act and was conducted under an investigational new drug approval by the U.S. Food and Drug Administration (investigational new drug application no. 133229). All participants rested for 1 hour before the study and moved to the scanner by means of a wheelchair. All MRI studies were performed with a 3.0-T MRI scanner (750w Discovery, GE Healthcare). The participant was placed

in the supine position with one leg in a ^{13}C -hydrogen 1 (^1H) dual-frequency radiofrequency coil for imaging the calf muscle (Fig 1, A–C). The cylindrical radiofrequency coil consisted of quadrature ^1H transmit-receive, ^{13}C quadrature transmit, and eight-channel ^{13}C array receiver coils (20). After resting MRI examinations, participants performed plantar flexion exercise (Fig 1, D), which activates PDH within 1 minute (3). HP examinations for exercising state involved plantar flexion exercise of calf muscle in the magnet using resistance bands (18,19). This protocol was chosen because PDH is rapidly activated with aerobic exercise (3). The participant began plantar flexion 1 minute before injection of HP pyruvate with a 3-second cycle for 3 minutes. For ^{13}C imaging with exercise, the participants were instructed to stop the exercise 3 seconds before the scanning started to suppress the motion artifacts. The ^{13}C images were obtained when the product HP signals peaked (ie, 33 seconds from the start of pyruvate injection) (Fig 2, E) to maximize the signal-to-noise ratio of products. For postexercise recovery examinations, the participant stood with the ball of the left foot on a 5-cm-thick block of wood and lifted himself or herself using plantar flexion and then returned to the resting position with the heel on the ground in a 2–3-second cycle for 60 seconds. Immediately after the exercise, participants were placed back in the scanner for postexercise scanning. Both exercise protocols were to activate the soleus and gastrocnemius (16,17).

Study participants were imaged using a ^{13}C - ^1H integrative MRI protocol, which consists of a series of ^1H MRI scans, including arterial spin labeling, and up to two sequential injections of HP $[1-^{13}\text{C}]$ -pyruvate at rest, during exercise, or 5 minutes after exercise (recovery). The second HP injection was performed 30 minutes after the first injection. Note that three HP ^{13}C data from participant 3 were acquired during two separate visits. A clinical dynamic nuclear polarization system (Spinlab, GE Healthcare) was used to produce HP $[1-^{13}\text{C}]$ -pyruvate (approximately 250 mmol/L) and the final injection was administered (0.4 mL/kg body weight) at a rate of 5 mL/sec, followed by a flush with 25 mL of saline. The general procedures were similar to those used in previous HP studies in human participants (10,11,21,22), and details of the protocol and data analysis are included in Appendix E1 (online). For ^{13}C MR spectroscopy, time-resolved free-induction-decay data were acquired using a section-selective pulse-and-acquire sequence. For ^{13}C MRI, a metabolite-selective multi-echo spiral imaging sequence was used to image $[^{13}\text{C}]$ -bicarbonate, $[1-^{13}\text{C}]$ -lactate, $[1-^{13}\text{C}]$ -pyruvate, and $[1-^{13}\text{C}]$ -alanine in an interleaved manner using a spectral-spatial radiofrequency pulse that selectively excites the labeled metabolites (23). The acquisition parameters are summarized in Table 2.

Statistical Analysis

All data analyses were performed with software (Excel, version 16.16.25, Microsoft). Data are reported as means \pm standard errors. Significance testing was conducted using the P value with two-tailed testing; $P < .05$ was considered a statistically significant difference. A paired t test was performed for comparing perfusion maps among the muscle states, and an unpaired t test was used for comparing ^{13}C data among the states.

Table 1: Study Participant Demographic Information

Participant No./Age (y)/Sex	Ethnicity	BMI (kg/m ²)	Height (cm)	Weight (kg)	Modality Used at Rest	Modality Used during Exercise	Modality Used at Recovery
1/28/M	Nonhispanic White	21.6	188.8	76.2	MRS	NA	MRS
2/65/F	Nonhispanic White	27.1	165.1	73.9	MRS	NA	MRS
3/62/M	Hispanic	26.4	160.0	67.5	MRS	MRS	MRS
4/18/F	Hispanic	24.2	154.9	58.1	ASL	MRS, ASL	NA
5/33/M	Hispanic	22.6	165.1	61.5	ASL	MRS, ASL	NA
6/34/M	Nonhispanic White	26.2	177.8	82.7	ASL	MRI, ASL	ASL
7/37/M	Nonhispanic White	20.3	173.0	60.9	MRI, ASL	MRI, ASL	NA
8/38/F	Nonhispanic White	18.4	172.7	54.9	ASL	NA	ASL
9/66/M	Nonhispanic White	26.4	185.4	90.0	ASL	NA	ASL

Note.—ASL = arterial spin labeling, BMI = body mass index, MRS = MR spectroscopy, NA = not available.

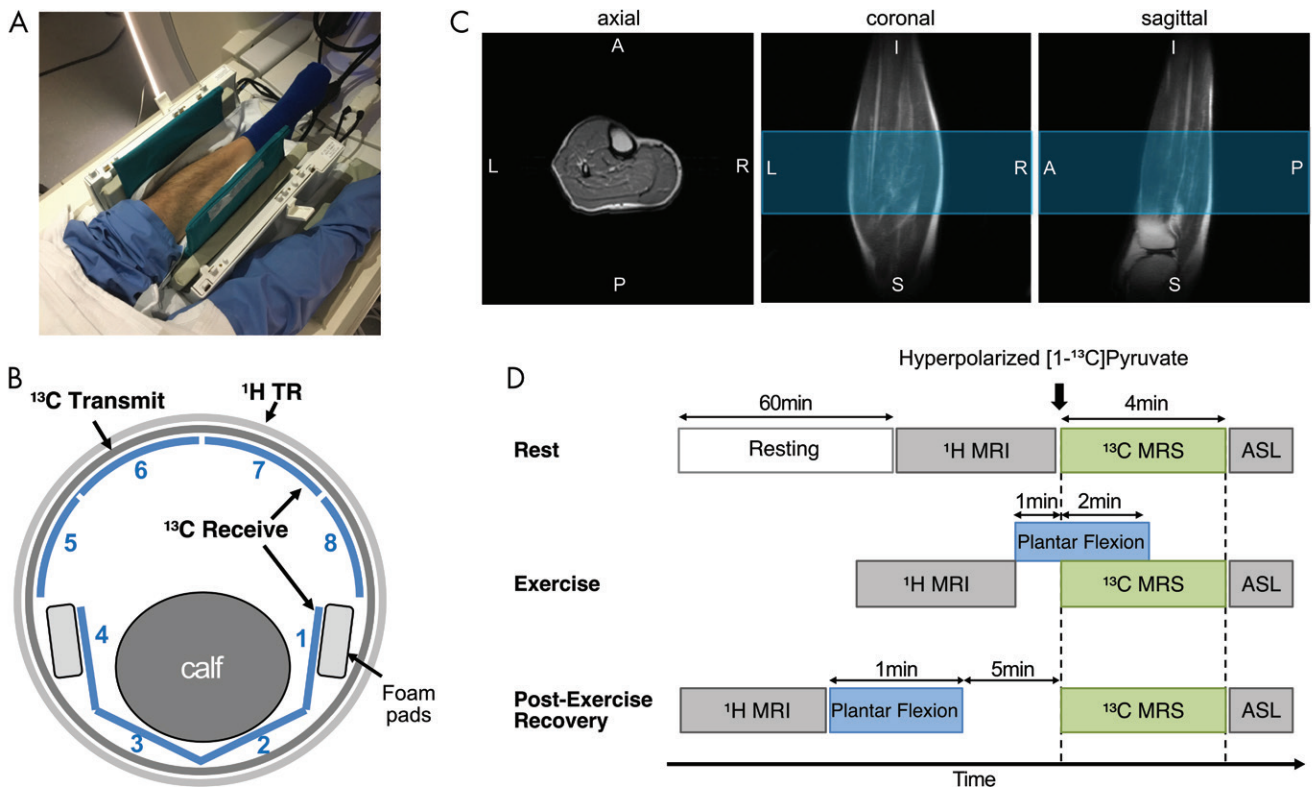


Figure 1: Experimental set-up and study protocol. A, Photograph depicts positioning of calf muscle in carbon 13 (¹³C)–hydrogen 1 (¹H) dual-frequency radiofrequency coil before connecting anterior part of coil. B, Illustration shows how calf muscle was wrapped with flexible posterior ¹³C array receiver coils (channels 1–4). TR = transmit and receive. C, Localized single-shot fast spin-echo ¹H MRI scans obtained using radiofrequency coil. Blue region indicates prescribed axial slab for ¹³C MR spectroscopy (10-cm thick). A = anterior, I = inferior, L = left, P = posterior, R = right, S = superior. D, Diagram shows how dynamic ¹³C MR spectroscopy (MRS) was performed at three metabolic states—rest, exercise, and recovery. ASL = arterial spin labeling.

Results

Examples of time-averaged ¹³C spectra and the time courses of HP metabolites from the three exercise conditions of participant 3 at rest, during exercise, and 5 minutes after exercise are shown in Figure 2. HP [¹³C]–bicarbonate, [¹⁻¹³C]–lactate, [¹⁻¹³C]–alanine, [¹⁻¹³C]–pyruvate hydrate, and [¹⁻¹³C]–pyruvate were detectable. The larger linewidth of ¹³C peaks in exercising muscle is probably due to the motion. The peak at 172.7 ppm is from natural abundance of ¹³C lipids and was confirmed with a baseline scan obtained without HP pyruvate injection (baseline

spectrum in Fig 2, A). Perfusion increased markedly after the exercises. Increased perfusion was confirmed with arterial spin labeling, which was performed at rest and immediately after postexercise HP scanning. Mean tissue perfusion increased from 17.1 mL/100 g/min ± 0.9 (standard error) at the resting state ($n = 6$) to 24.0 mL/100 g/min ± 2.1 ($n = 4$, $P = .02$) with exercise and to 27.6 mL/100 g/min ± 2.4 ($n = 3$, $P = .03$) during recovery (Fig 3, A). Total HP ¹³C signals (tC), adjusted with polarization parameters, increased to 2.8-fold of that of the resting state ($n = 3$) with exercise ($n = 3$, $P = .005$) and to 3.2-fold during recovery

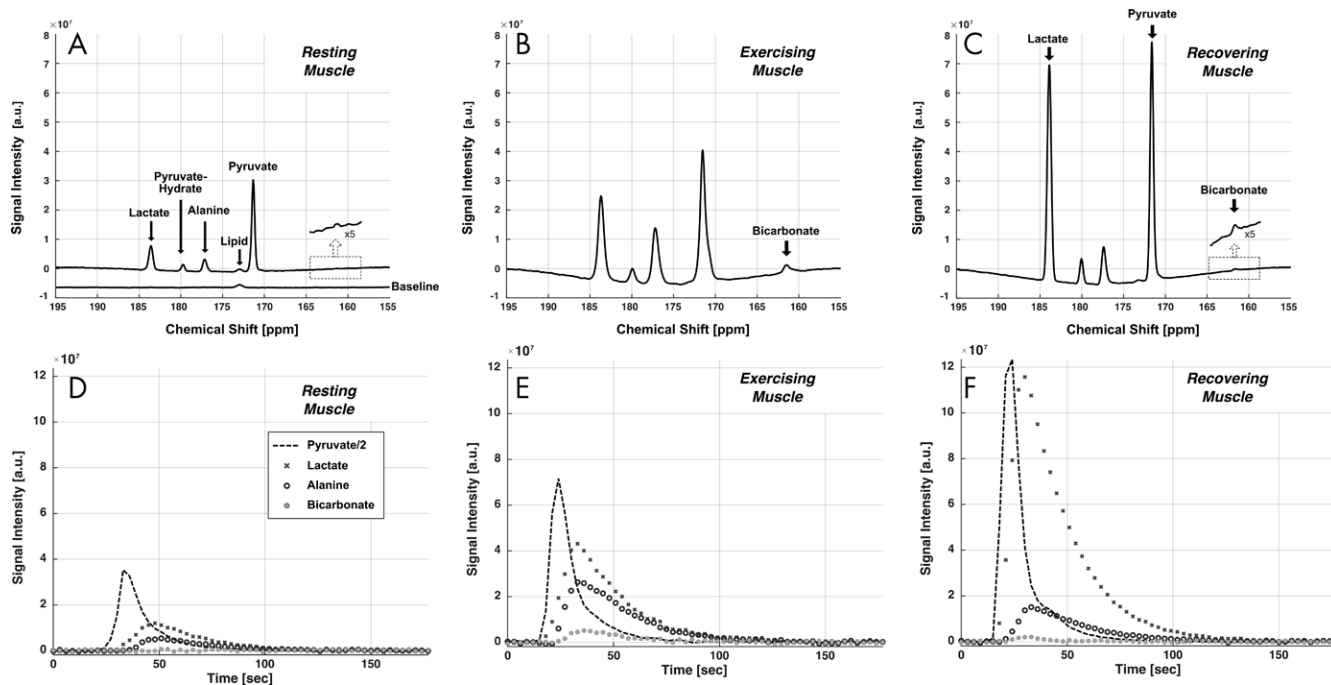


Figure 2: Carbon 13 (^{13}C) spectra and time courses of ^{13}C metabolites acquired at rest and with exercise using hyperpolarized (HP) [$1\text{-}^{13}\text{C}$]-pyruvate. a.u. = arbitrary units. A–C, ^{13}C spectra were averaged during the first 90 seconds after a bolus injection of HP [$1\text{-}^{13}\text{C}$]-pyruvate in 62-year-old man (participant 3), A, at rest, B, during plantar flexion exercise, and, C, during postexercise recovery. Peak at 172.7 ppm is from natural abundance of ^{13}C lipids. D–F, Time courses of HP ^{13}C metabolites. Time-resolved [$1\text{-}^{13}\text{C}$]-pyruvate (dashed line), [$1\text{-}^{13}\text{C}$]-lactate (X), [$1\text{-}^{13}\text{C}$]-alanine (open circle), and [^{13}C]-bicarbonate (gray circle) from participant, D, at rest, E, during exercise, and, F, during postexercise recovery.

Table 2: MRI Acquisition Parameters

Parameter	Three-dimensional ^1H PCASL	Two-dimensional ^1H T2-weighted FSE	Dynamic ^{13}C MRS	Two-dimensional ^{13}C MESI
Image orientation	Axial	Axial	Axial	Axial
Repetition time (msec)	5366	5000	3000	117
No. of echoes	1	2	NA	6
Echo times (msec)	9.9	11.3, 65.0	NA	12.2, 18.2, 24.1, 30.1, 36.1, 42.1
Echo train length	1	8	NA	1
No. of signals acquired	3	1	80	1
Flip angle (degrees)	111	160	11.25	20, 90, 90, 90
Section thickness (mm)	6	10	100	80
Field of view (mm)	240	240	NA	240
Acquisition matrix	512 points per spiral arm \times 8 arms	192 \times 192	2048 (spectral) \times 80 (time)	1492 point per spiral arm \times 1 arm per metabolite \times 4 metabolites
Reconstruction matrix	128 \times 128	256 \times 256	8192 \times 80	64 \times 64 per metabolite \times 4 metabolite
Sections	21	8	1	1
Acquisition time	6 minutes 15 seconds	6 minutes 10 seconds	4 minutes	<0:01 minute
Other parameters	Postlabeling delay = 3025 msec	NA	Spectral width = 10 000 Hz	Acquisition order: bicarbonate, lactate, alanine, and pyruvate

Note.— ^{13}C = carbon 13, FSE = fast spin echo, ^1H = hydrogen 1, MESI = multi-echo spiral imaging, MRS = MR spectroscopy, NA = not applicable, PCASL = pseudocontinuous arterial spin labeling.

ery ($n = 3$, $P = .10$). Total [$1\text{-}^{13}\text{C}$]-pyruvate signals, normalized with tC, at rest (mean, 0.66 ± 0.03) were higher than those measured during exercise (mean, 0.41 ± 0.03 ; $P = .003$) or recovery (mean, 0.45 ± 0.02 ; $P = .005$). Total [$1\text{-}^{13}\text{C}$]-lactate signals (lactate-to-tC ratio) produced from HP [$1\text{-}^{13}\text{C}$]-pyruvate were

higher during the recovery period (mean, 0.42 ± 0.03) than during rest (mean, 0.18 ± 0.04 ; $P = .008$) and during exercise (mean, 0.31 ± 0.02 ; $P = .04$). Normalized alanine production (alanine-to-tC ratio) was highest during exercise (mean, 0.22 ± 0.02) than during recovery (mean, 0.11 ± 0.02 ; $P = .03$)

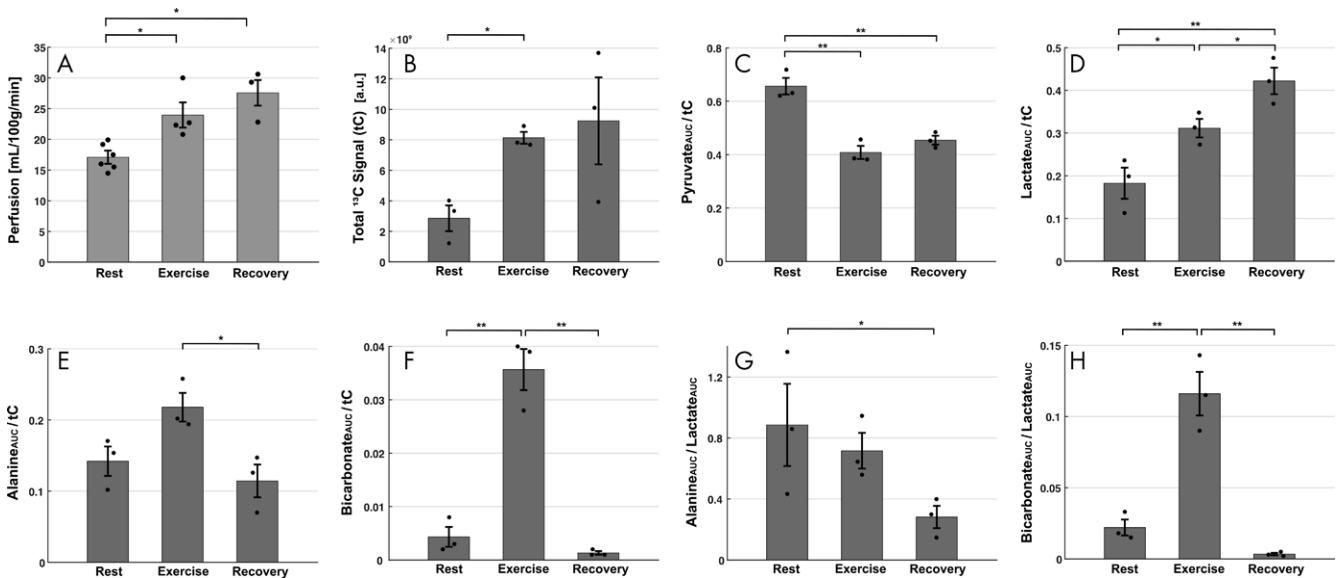


Figure 3: Bar graphs show effect of exercise in hyperpolarized carbon 13 (^{13}C) MR spectroscopy. Data are means \pm standard errors. * indicates $P < .05$, and ** indicates $P < .01$. A, Spatially averaged perfusion measured with hydrogen 1 (^1H) arterial spin labeling from participants at rest ($n = 6$), during exercise ($n = 4$), and during recovery ($n = 3$). B, Total ^{13}C signals (tC) after adjusting difference in polarization and experimental parameters (three participants per group). a.u. = arbitrary units. C–F, Area under the curve (AUC) for, C, [$1\text{-}^{13}\text{C}$]-pyruvate, D, [$1\text{-}^{13}\text{C}$]-lactate, E, [$1\text{-}^{13}\text{C}$]-alanine, and, F, [^{13}C]-bicarbonate, normalized with tC area under the curve. G, H, Area under the curve (AUC) of, G, alanine and, H, bicarbonate, normalized with lactate area under the curve.

or rest (mean, 0.14 ± 0.02 ; $P = .06$). Exercise produced more bicarbonate (bicarbonate-to-tC ratio) (mean, 0.036 ± 0.004) than rest (mean, 0.004 ± 0.002 ; $P = .002$) or recovery (mean, 0.002 ± 0.001 ; $P = .001$). The alanine-to-lactate ratio further decreased during recovery (mean, 0.28 ± 0.07) from that measured during exercise (mean, 0.72 ± 0.12 ; $P = .03$). The bicarbonate-to-lactate ratio during exercise (mean, 0.036 ± 0.004) was higher than that in resting (mean, 0.004 ± 0.002 ; $P = .004$) and recovering (mean, 0.002 ± 0.001 ; $P = .002$) states.

To confirm the source of HP ^{13}C signals, two-dimensional images of calf muscle were obtained in two healthy participants (participants 6 and 7) during exercise as shown in Figure 4. From both participants, [$1\text{-}^{13}\text{C}$]-pyruvate, [$1\text{-}^{13}\text{C}$]-lactate, [$1\text{-}^{13}\text{C}$]-alanine, and [^{13}C]-bicarbonate maps were obtained with the exercise, and the HP signals were primarily from the medial and lateral gastrocnemius. High [$1\text{-}^{13}\text{C}$]-pyruvate signals were also detected from the blood vessels. At rest, the product images were at the noise level.

Discussion

In this study, we demonstrated that hyperpolarized (HP) [$1\text{-}^{13}\text{C}$]-pyruvate is sensitive to the exercise state of skeletal muscle in humans. Using in-magnet plantar flexion exercise, real-time pyruvate dehydrogenase (PDH) and lactate dehydrogenase activities could be monitored. Separate scanning with HP pyruvate evaluated pyruvate metabolism at rest or during recovery. As a fraction of total HP ^{13}C signals (tC), both protocols were associated with an increase in HP [$1\text{-}^{13}\text{C}$]-lactate-to-tC ratio (1.7-fold increase during exercise, $P = .005$; 2.3-fold increase during recovery, $P = .008$). The increase of bicarbonate during exercise ($P = .002$) directly indicates activation of PDH, and the disappearance of bicarbonate after exercise suggests rapid deactivation of PDH during the recovery

period. These patterns were highly reproducible from different participants (Fig 3, D, F).

Intravenously injected HP pyruvate is rapidly distributed to each organ by means of arterial inflow and subsequently enters the interstitial space, followed by transport into the cytosol. In skeletal muscle, approximately 15% of tissue volume is occupied by interstitial and vascular compartments (24). Consequently, the majority of the observed products must originate from intracellular metabolites. Although lactate is often described as a product of metabolism during hypoxic or ischemic conditions, it is normally present in low concentration in muscle under resting and well-oxygenated conditions. Because of its low concentration, lactate is not detected in skeletal muscle at rest with ^1H MR spectroscopy, yet lactate was readily observed in resting skeletal muscle in this study, indicating exchange of [$1\text{-}^{13}\text{C}$]-pyruvate into the existing lactate pool and the high sensitivity of HP methods. A substantial increase in HP [$1\text{-}^{13}\text{C}$]-lactate was detected during exercise and recovery and correlated with an increase in perfusion, consistent with earlier results from ^1H MR spectroscopy (25). Similarly, alanine production regulated by alanine aminotransferase is affected by the intrinsic alanine pool size and also by the balance between lactate dehydrogenase and alanine aminotransferase activities. The decreased postexercise HP [$1\text{-}^{13}\text{C}$]-alanine level relative to the [$1\text{-}^{13}\text{C}$]-lactate level suggests the use of alanine as an index of intracellular delivery of pyruvate in skeletal muscle.

Unlike products of exchange reactions, such as [$1\text{-}^{13}\text{C}$]-lactate and [$1\text{-}^{13}\text{C}$]-alanine, [^{13}C]-bicarbonate directly indicates pyruvate flux into acetyl coenzyme A by means of PDH, and the amount of HP bicarbonate from HP pyruvate is proportional to PDH flux. The short in-magnet exercise before HP injection activated PDH flux in skeletal muscle, as would be expected if glycogen provided all necessary acetyl coenzyme A. Because of intracellular compartmentation of glycogen and relevant enzymes,

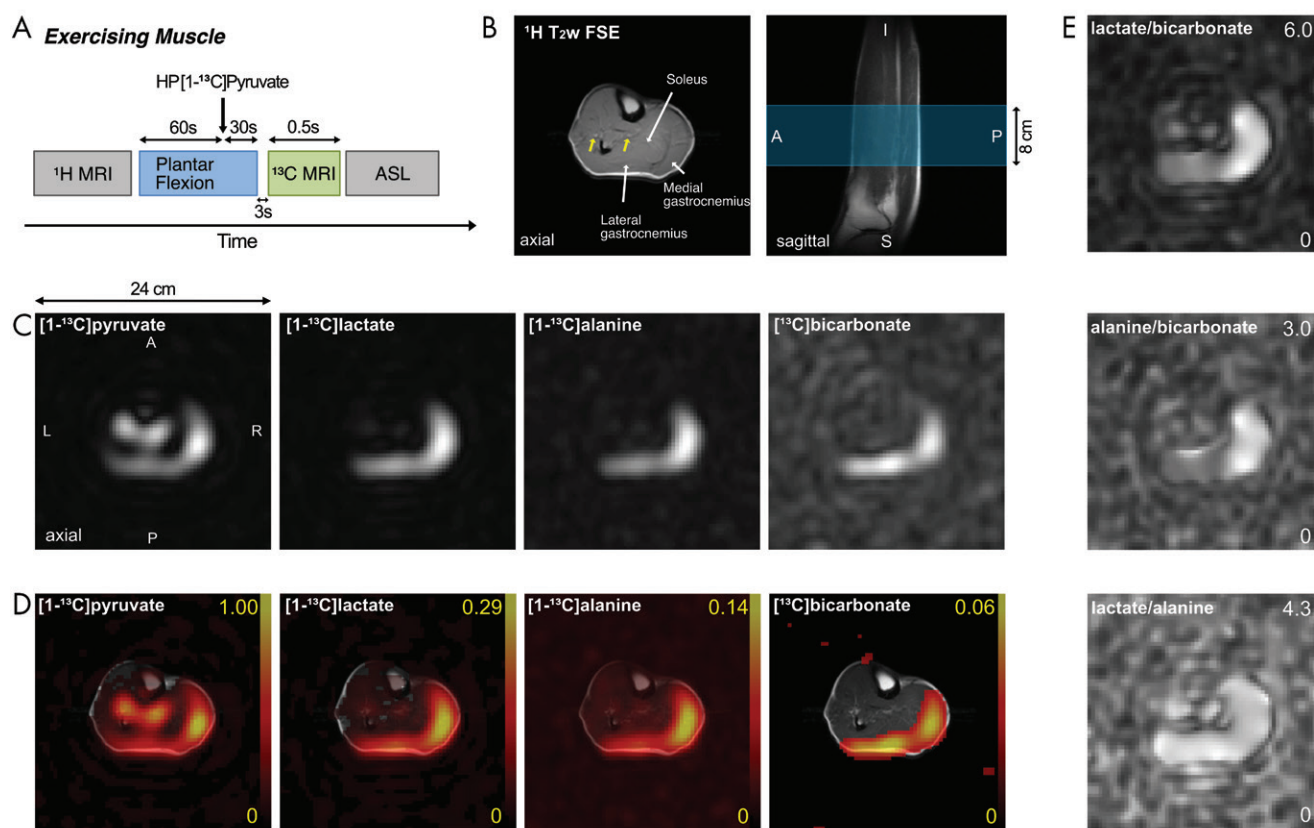


Figure 4: Metabolic imaging of calf muscle with exercise. A, Diagram shows how hyperpolarized (HP) carbon 13 (^{13}C) MRI was performed in exercising muscle. ASL = arterial spin labeling, ^1H = hydrogen 1. B, ^1H T2-weighted (T2w) fast spin-echo (FSE) MRI scan of 8-cm axial section in study participant 6 (34-year-old man). Blue region in sagittal MRI scan indicates prescribed axial section for ^{13}C MRI. Yellow arrows indicate arteries. A = anterior, I = inferior, P = posterior, S = superior. C, Time-averaged metabolite maps of hyperpolarized [^{1-13}C]-pyruvate, [^{1-13}C]-lactate, [^{1-13}C]-alanine, and [^{13}C]-bicarbonate. A = anterior, L = left, P = posterior, R = right. D, ^{13}C metabolite maps, normalized with peak [^{1-13}C]-pyruvate signal and overlaid on corresponding hydrogen 1 fast spin-echo image of section. E, Metabolite ratio maps of carbon 13 products—lactate-to-bicarbonate ratio, alanine-to-bicarbonate ratio, and lactate-to-alanine ratio.

glycogen is the predominant source of energy production early in exercise (12,26). The contribution of blood-borne substrates to energy production is quite difficult to study in human participants because of the requirement for invasive measures of arteriovenous content differences plus measurements of perfusion, which are difficult to achieve in exercising muscle. Because PDH is integral to carbohydrate metabolism, the HP method enables the investigation of both normal physiologic findings and exercise training and study of numerous disorders. Furthermore, the HP examination is relatively brief. Thus, integration with ^1H and phosphorus 31 (^{31}P) MR spectroscopy is practical. The negligible [^{13}C]-bicarbonate during the recovery can arise from the accumulation of high concentrations of acetylcarnitine during exercise, which now buffers the acetyl coenzyme A demand during recovery, as described earlier (17). The muscle does not need additional acetyl coenzyme A to support energy production. HP experiments can readily test such a hypothesis involving acetylcarnitine (14).

Our study had limitations. First, spatial heterogeneity of the skeletal muscle was not considered. Muscle compartments, such as those in the gastrocnemius and soleus, consist of different distributions of fast-twitch glycolytic fibers and slow-twitch oxidative fibers, which present wide ranges of enzyme activities and contractile properties (27,28). The distinct metabolic profiles between

the medial and lateral gastrocnemius suggest that compartmentalized comparison is necessary for accurate metabolic assessment of exercising muscle. More quantitative assessment can be achieved by distinguishing muscle fiber distributions in ^1H MRI or by obtaining volumetric ^{13}C images. Second, discrepancies in duration, timing, and types of the plantar flexion exercise between the studies (eg, exercising vs recovery and MR spectroscopy vs MRI) potentially contribute as additional variables to the results. Third, the ^{13}C images were acquired immediately (approximately 3 seconds) after the exercise to minimize the motion artifacts. The image acquisition was instantaneous (<0.5 second), but the imaging data were acquired technically during the early phase of recovery. Because the acute metabolic changes after termination of exercise are crucial elements for quantitative interpretation of skeletal muscle physiologic findings, future studies need to consider imaging during the exercise to avoid potential complication.

The HP approach complements other MR methods in examining the enzymatic response to exercise and recovery in skeletal muscle and, in principle, should be useful in understanding conditions associated with ischemia. In contrast to dynamic contrast-enhanced MRI or arterial spin labeling, which assesses oxygen delivery according to images of blood perfusion, HP pyruvate MR spectroscopy focuses on the enzyme activity in critical

metabolic steps controlling oxidative phosphorylation, such as PDH activity. For example, ³¹P phosphocreatine recovery kinetics after exercise reflect the overall mitochondrial bioenergetics under exercise conditions and specifically help detect carbohydrate oxidation. Combining different MR techniques would lead to a more comprehensive understanding of exercise, muscle ischemia, and other conditions.

In conclusion, the experiments demonstrated the feasibility of measuring pyruvate metabolism of skeletal muscle using hyperpolarized (HP) [1-carbon ¹³C]-pyruvate in response to exercise. Imaging the products of HP [1-¹³C]-pyruvate, such as lactate, alanine, and bicarbonate, during exercise provides a direct assessment of pyruvate metabolism and flux in key enzymes. In particular, HP MRI presents then a unique approach to measure pyruvate dehydrogenase (PDH) flux directly in skeletal muscle under different physiologic conditions. Hence, the HP approach offers a way to study PDH activation and regulation in human skeletal muscle, thus opening a new frontier for noninvasive assessment of muscle physiologic characteristics. Practical applications of HP [1-¹³C]-pyruvate include peripheral vascular (arterial) disease and myopathy that may result in muscle ischemia or excessive anaerobic metabolism for early noninvasive diagnosis and follow-up after treatment. For this, quantitative imaging biomarkers that reflect physiologic conditions of the skeletal muscle need to be identified, and proper analytical methods should be established.

Author contributions: Guarantors of integrity of entire study, J.M.P., C.R.M.; study concepts/study design or data acquisition or data analysis/interpretation, all authors; manuscript drafting or manuscript revision for important intellectual content, all authors; approval of final version of submitted manuscript, all authors; agrees to ensure any questions related to the work are appropriately resolved, all authors; literature research, J.M.P., J.C., T.J., C.R.M.; clinical studies, J.M.P., C.E.H., J.L., G.D.R., C.R.M.; statistical analysis, J.M.P.; and manuscript editing, J.M.P., C.E.H., J.M., J.C., Z.Z., A.C., R.G.H., T.J., C.R.M.

Acknowledgments: The authors appreciate Jeannie Baxter, RN, Kelley Derner, RN, Maida Tai, and Salvador Peña, RT(R)(MR), for recruiting and imaging the volunteers.

Disclosures of Conflicts of Interest: J.M.P. disclosed no relevant relationships. C.E.H. disclosed no relevant relationships. J.M. disclosed no relevant relationships. J.C. disclosed no relevant relationships. J.R. disclosed no relevant relationships. Z.Z. disclosed no relevant relationships. J.L. Activities related to the present article: disclosed no relevant relationships. Activities not related to the present article: is a medical science liaison with AstraZeneca; holds stock/stock options in AstraZeneca. Other relationships: disclosed no relevant relationships. G.D.R. Activities related to the present article: disclosed no relevant relationships. Activities not related to the present article: is employed with GE Healthcare. Other relationships: disclosed no relevant relationships. A.C. Activities related to the present article: disclosed no relevant relationships. Activities not related to the present article: is a consultant for ICON Medical and Treace 3D Medical Concepts; receives royalties from Wolters and Jaypee. Other relationships: disclosed no relevant relationships. R.G.H. disclosed no relevant relationships. T.J. disclosed no relevant relationships. C.R.M. disclosed no relevant relationships.

References

- Hargreaves M, Spriet LL. Skeletal muscle energy metabolism during exercise. *Nat Metab* 2020;2(9):817–828 [Published correction appears in *Nat Metab* 2020;2(9):990.] <https://doi.org/10.1038/s42255-020-0251-4>.
- Kasper JD, Meyer RA, Beard DA, Wiseman RW. Effects of altered pyruvate dehydrogenase activity on contracting skeletal muscle bioenergetics. *Am J Physiol Regul Integr Comp Physiol* 2019;316(1):R76–R86.
- Spriet LL, Heigenhauser GJF. Regulation of pyruvate dehydrogenase (PDH) activity in human skeletal muscle during exercise. *Exerc Sport Sci Rev* 2002;30(2):91–95.
- Consitt LA, Saxena G, Saneda A, Houmar JA. Age-related impairments in skeletal muscle PDH phosphorylation and plasma lactate are indicative of metabolic inflexibility and the effects of exercise training. *Am J Physiol Endocrinol Metab* 2016;311(1):E145–E156.
- Kelley DE, Mokan M, Mandarino LJ. Intracellular defects in glucose metabolism in obese patients with NIDDM. *Diabetes* 1992;41(6):698–706.
- Patel KP, O'Brien TW, Subramony SH, Shuster J, Stacpoole PW. The spectrum of pyruvate dehydrogenase complex deficiency: clinical, biochemical and genetic features in 371 patients. *Mol Genet Metab* 2012;106(3):385–394.
- Stenlid MH, Ahlsson F, Forslund A, von Döbeln U, Gustafsson J. Energy substrate metabolism in pyruvate dehydrogenase complex deficiency. *J Pediatr Endocrinol Metab* 2014;27(11-12):1059–1064.
- DeBrosse SD, Okajima K, Zhang S, et al. Spectrum of neurological and survival outcomes in pyruvate dehydrogenase complex (PDC) deficiency: lack of correlation with genotype. *Mol Genet Metab* 2012;107(3):394–402.
- Gastin PB. Energy system interaction and relative contribution during maximal exercise. *Sports Med* 2001;31(10):725–741.
- Nelson SJ, Kurhanewicz J, Vigneron DB, et al. Metabolic imaging of patients with prostate cancer using hyperpolarized [1-¹³C]pyruvate. *Sci Transl Med* 2013;5(198):198ra108.
- Cunningham CH, Lau JY, Chen AP, et al. Hyperpolarized ¹³C metabolic MRI of the human heart: initial experience. *Circ Res* 2016;119(11):1177–1182.
- van Loon LJ, Greenhaff PL, Constantin-Teodosiu D, Saris WH, Wagenmakers AJ. The effects of increasing exercise intensity on muscle fuel utilisation in humans. *J Physiol* 2001;536(Pt 1):295–304.
- Henriksson J. Muscle fuel selection: effect of exercise and training. *Proc Nutr Soc* 1995;54(1):125–138.
- Park JM, Josan S, Mayer D, et al. Hyperpolarized ¹³C NMR observation of lactate kinetics in skeletal muscle. *J Exp Biol* 2015;218(Pt 20):3308–3318.
- Leftin A, Roussel T, Frydman L. Hyperpolarized functional magnetic resonance of murine skeletal muscle enabled by multiple tracer-paradigm synchronizations. *PLoS One* 2014;9(4):e96399.
- Bansal N, Szczepaniak L, Ternullo D, Fleckenstein JL, Malloy CR. Effect of exercise on (23)Na MRI and relaxation characteristics of the human calf muscle. *J Magn Reson Imaging* 2000;11(5):532–538.
- Ren J, Lakoski S, Haller RG, Sherry AD, Malloy CR. Dynamic monitoring of carnitine and acetylcarnitine in the trimethylamine signal after exercise in human skeletal muscle by 7T 1H-MRS. *Magn Reson Med* 2013;69(1):7–17.
- Parasoglou P, Xia D, Chang G, Regatte RR. Dynamic three-dimensional imaging of phosphocreatine recovery kinetics in the human lower leg muscles at 3T and 7T: a preliminary study. *NMR Biomed* 2013;26(3):348–356.
- Sleigh A, Lupson V, Thankamony A, et al. Simple and effective exercise design for assessing in vivo mitochondrial function in clinical applications using (31)P magnetic resonance spectroscopy. *Sci Rep* 2016;6(1):19057–19059.
- Ma J, Hashoian RS, Sun C, et al. Development of 1H/13C RF head coil for hyperpolarized ¹³C imaging of human brain [abstr]. In: Proceedings of the Twenty-Seventh Meeting of the International Society for Magnetic Resonance in Medicine. Berkeley, Calif: International Society for Magnetic Resonance in Medicine, 2019; 568.
- Rider OJ, Apps A, Miller JJ, et al. Noninvasive In Vivo Assessment of Cardiac Metabolism in the Healthy and Diabetic Human Heart Using Hyperpolarized ¹³C MRI. *Circ Res* 2020;126(6):725–736.
- Park JM, Reed GD, Liticker J, et al. Effect of Doxorubicin on Myocardial Bicarbonate Production from Pyruvate Dehydrogenase in Women with Breast Cancer. *Circ Res* 2020;127(12):1568–1570.
- Ma J, Chen J, Reed GD, et al. Cardiac T*2 measurement of hyperpolarized ¹³C metabolites using metabolite-selective multi-echo spiral imaging. *Magn Reson Med* 2021. 10.1002/mrm.28796. Published online April 6, 2021.
- Levitt DG. The pharmacokinetics of the interstitial space in humans. *BMC Clin Pharmacol* 2003;3(1):3–29.
- Meyerspeer M, Kemp GJ, Mlynárik V, et al. Direct noninvasive quantification of lactate and high energy phosphates simultaneously in exercising human skeletal muscle by localized magnetic resonance spectroscopy. *Magn Reson Med* 2007;57(4):654–660.
- Ørtenblad N, Nielsen J. Muscle glycogen and cell function—Location, location, location. *Scand J Med Sci Sports* 2015;25(Suppl 4):34–40.
- Moss CL. Comparison of the histochemical and contractile properties of human gastrocnemius muscle. *J Orthop Sports Phys Ther* 1991;13(6):322–328.
- Gollnick PD, Sjödin B, Karlsson J, Jansson E, Saltin B. Human soleus muscle: a comparison of fiber composition and enzyme activities with other leg muscles. *Pflügers Arch* 1974;348(3):247–255.